

Study on the breaking span and the influence on gas migration in goaf

To solve the abnormal gas emission of goaf during the thick coal seam overlying hard roof to pressure on the Tashan coal Mine in Datong, focusing on the hard roof of some working surface in Datong mining, and based the key stratum theory, Vlasov thick plate theory and thin plate theory, this paper gets the breaking span of hard rock strata which are quite different in thickness in a near distance, and explains the stratum caving with different weighting. We established the dynamic, migration model of gas in the mined out area under the impact of collapse according to the characteristics of overlying strata, with the aid of COMSOL multi-physical field coupling software, to analyze the gas emission law in the goaf under the overlying stratum. The result shows that the breaking span of the upper roof is twice longer than the lower one, leading to strong and weak weighting. When the layered roof rock caving, the most of mining goaf gas will be poured into the working face upper corner and the high extracted way. Especially in the upper roof caving, the upper corner gas concentration increases obviously. So the goaf and the upper corner gas should be the focus of governance.

Keywords: hard roof, thick plate theory, layered fracture, goaf gas, dynamic migration

1. Introduction

The coal seam of Tashan coal Mine in Datong in China is special thick, but the content of adsorption methane is low [1]. The mining roof is the most typical hard and difficult caving roof at home and abroad. The goaf extrusion disturbance which was caused by the movement of overlying strata in mining area leads to abnormal gas emission there. Sogas overrun phenomenon occurs in the working face sometimes, and it affects mine safety production. Therefore, it has important significance to study the roof breaking characteristics and the research of gas migration in goaf under

roof caving[2-4].

The research of overlying strata movement in mining field is also based on the theory of “beam” and “slab”, but the Datong mining area owns a hard roof with thick layer, and the roof span is larger. So the characteristics of mechanical model cannot meet the research and calculation of the broken step distance of thick layer of hard roof(hard roof with thick layer). Therefore, it has important significance to study the roof caving step distance of Datong Mining Area with the help of the “board” theory [5-6]. According to the “board” theory, Jia Xirong [7]established the theory of mining pressure, Tang Xiaoling[8] calculated the initial stage and the period of the thin seam roof, And Tu Hongsheng [9] studied the characteristics of the initial deformation and fracture of the roof of the steeply inclined working face based on the thin plate theory.For the characteristics of Datong mining thin roof and thick roof there, the use of thin plate theory and thick plate theory combination becomes the key of study. The gob extrusion disturbance is produced by roof caving to the mining area, which causes the abnormal gas emission, and the roof caving of different rock strata makes different influence on the gas emission in goaf. Weng Mingyue[10] took the experimental study in Tunliu Coal Mine S2205 held on working face of the fracture of coal or rock micro-seismic monitoring, working face of mine pressure behavior monitoring and gas emission, and got the relationship among the fully mechanized caving face of coal rock, strata pressure and gas emission. Li Huamin[11] used #13 coal mine 12071 working face as an example, real-time monitored the support resistance, the abutment pressure and the working face of the gas volume fraction, analyzed the relationship between the process of mining and gas emission.

However, at present, the research on the static flow field is mainly based on the working face in normal environment, and there is few researches of the dynamic gas migration under different roof caving step distance. So, the relationship between roof activity and gas emission could not be correctly reflected. In this work, based on the collapse characteristics of overburden strata and the gas flow theory in porous media, the dynamic migration model of goaf under different caving step impact was established, and the law of gas emission from

Messrs. Binwei Xia, Shijie Guo, Yiyu Lu, Xiaolong Li, Peng Yu and Jinlong Jia, State Key Laboratory for Coal Mine Disaster Dynamics and Control, Chongqing University, Chongqing 400044, China; National and Local Joint Engineering Laboratory of Gas Drainage in Complex Coal Seam, Chongqing University, Chongqing 400044, China. Email:20097177@cqu.edu.cn

goaf was analyzed, and the basis for preventing and controlling mine gas disaster was provided.

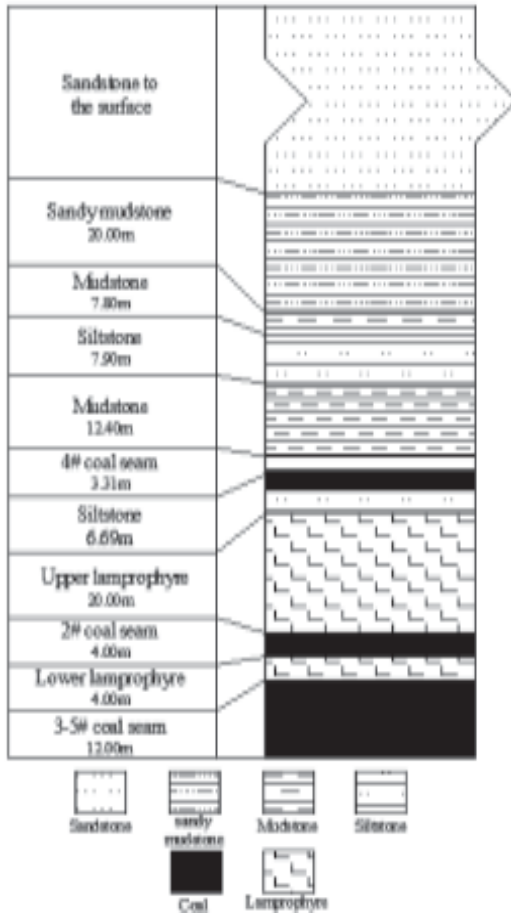


Fig.1 The photograph of rock column

2. Engineering summary

A mining working face of Tashan Coal Mine in Datong is the main research object. The thick of 3~5# coal seam average is 12 meters, its coal seam inclination is 3 degrees, and it is a nearly horizontal thick coal seam. The mine fully mechanized caving low caving coal once mining full height method was used, and its mining thickness was 3.5 meters, coal thickness was 8.5 meters, working face advance speed was 5.6m/d. One

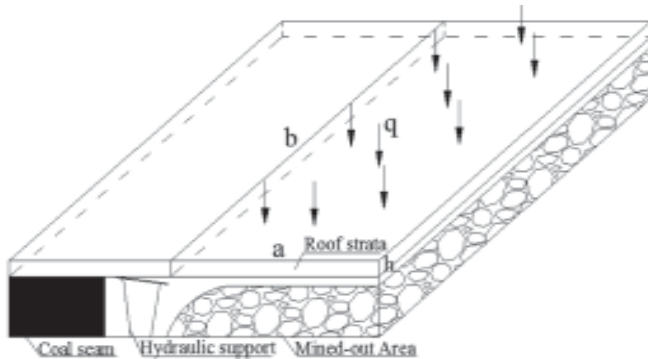


Fig.2 Stress diagram of simple-supported rectangular plate

inlet and two back ventilation mode was adopted, inlet air was 3600m³/min, return air was 2400m³/min, high exhaust quantity was 1200m³/min.

3-5# roof exists near distance and the large thickness difference between the larger lamprophyres, its lower lamprophyre thickness is 4 meters, upper lamprophyre thickness is 20 meters. There is 2# seam of 4m between the two layers of lamprophyre. Lamprophyre Platts hardness is a hard rock as IV, the top and bottom strata histogram is shown as Fig.1.

3. Roof caving step distance study

As the roof of the mining field is a flat plate, the roof boundary condition could be changed into four edges simply supported with the advancing of the mining face. The roof can be simplified to the rectangular plate with four edges simply, in considering of the simplicity and accuracy of the calculation. And the thickness of the plate is h .

Plates can be divided into thin, thick, and thin films. The criterion is given as follows:

Thin plate:

$$\left(\frac{1}{80} \sim \frac{1}{100}\right) \leq \frac{h}{a} \leq \left(\frac{1}{5} \sim \frac{1}{8}\right) \quad \dots 1$$

Thick plate:

$$\frac{h}{a} > \left(\frac{1}{5} \sim \frac{1}{8}\right) \quad \dots 2$$

Thin film:

$$\frac{h}{a} < \left(\frac{1}{80} \sim \frac{1}{100}\right) \quad \dots 3$$

The width of working face is 230 meters. The upper lamprophyre thickness is 20m, in-situ caving step is 60 to 70 meters, so the short side length is 60 to 70 meters. As $\frac{h}{a} = \frac{20}{60 \sim 70} > \frac{1}{5}$, the thick plate theory has been taken to calculate the fracture step distance. The lower lamprophyre thickness is 4 meters, caving distance is 35 to 40 meters, so the short side length is 35 to 40 meters, As $\frac{h}{a} = \frac{4}{35 \sim 40} < \frac{1}{8}$, the thin plate theory has been taken to compute the fracture step distance .

The key strata theory [12] shows that 4 meters thick hard lower lamprophyres are regarded as a sub key layer. And the thick and hard upper lamprophyre 20 meters above it is regarded as a sub key layer, too. The histogram shows that the surface with a siltstone rock whose thickness is up to tens meters. The siltstone rock is high integrity, but the stratification is not obvious. So it is regarded as the main key stratum. Assume that S1 is the first layer of key layer, then load on it is given by:

$$q = \frac{E_i h_i^3 \sum_{i=1}^n \gamma_i h_i}{\sum_{i=1}^n E_i h_i^3} \quad \dots 4$$

In the formula, the E_i is the elastic modulus of the i layer; h_i is the thickness of the i layer; γ_i is the bulk density of layer; is the rock layers controlled by the key layer; So, q is the weight load of all controlled rock strata. Then the mechanical model of roof strata is shown in Fig.3.

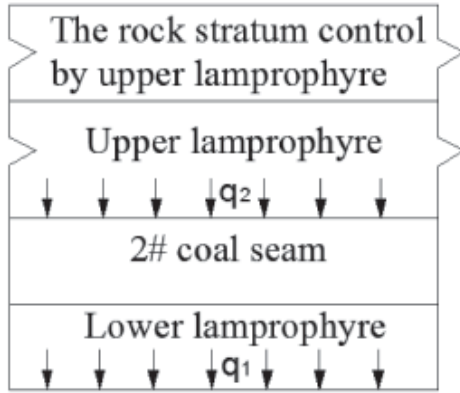


Fig.3 The mechanical model of roof strata

Where q_1 is the load per unit area of the lower lamprophyre, q_2 is the load per unit area of the upper lamprophyre. According to the strata histogram and key layer theory, it can be got that the control of upper lamprophyre height is 54.1 meters, the control of lower lamprophyre is 2# seam thickness, it is 4 meters.

Using formula (1) based on the mechanical parameters of coal rock, it can be calculated that: $q_1 = 0.158MPa$ and $q_2 = 1.85MPa$.

3.1 THE UPPER LAMPROPHYRE CAVING STEP

The Vlasov theory [13] considering the transverse shear deformation is a precise thick plate theory, and it is widely used in shell strength calculation and dynamic analysis.

Based on the assumption that the true displacement of each point on the middle plane normal after the transverse shear deformation is a nonlinear distribution, the relationship between the shear stress and the displacement is given by:

$$\tau_{yz} = \frac{E}{2(1+\mu)} \left(\frac{\partial v}{\partial z} + \frac{\partial \omega}{\partial y} \right), \quad \dots 5$$

From the above two formulas, the angle of Kirchhoff in the surface can be written as:

$$\varphi_x = \frac{\partial \omega}{\partial x} - \frac{\tau_{xz}^0}{G}, \quad \varphi_y = \frac{\partial \omega}{\partial y} - \frac{\tau_{yz}^0}{G} \quad \dots 6$$

The boundary conditions of simply supported rectangular plates at four sides are given by:

$$\text{At the } x = 0 \text{ and } x = a, \quad \omega = 0, \quad \varphi_x = 0, \quad M_x = 0$$

$$\text{At the } y = 0 \text{ and } y = b, \quad \omega = 0, \quad \varphi_y = 0, \quad M_y = 0 \quad \dots 7$$

Using the formula (6), the internal force of Vlasov can be written as:

$$M_x = -\frac{D}{5} \left[4 \left(\frac{\partial \varphi_x}{\partial x} + \mu \frac{\partial \varphi_y}{\partial y} \right) + \left(\frac{\partial^2 \omega}{\partial x^2} + \mu \frac{\partial^2 \omega}{\partial y^2} \right) \right]$$

$$M_y = -\frac{D}{5} \left[4 \left(\frac{\partial \varphi_y}{\partial y} + \mu \frac{\partial \varphi_x}{\partial x} \right) + \left(\frac{\partial^2 \omega}{\partial y^2} + \mu \frac{\partial^2 \omega}{\partial x^2} \right) \right] \quad \dots 8$$

At the same time, the differential equations of thick plate are rewritten as:

$$\frac{2D}{5} \left[(1-\mu) \nabla^2 \varphi_x + (1+\mu) \frac{\partial \phi}{\partial x} + \frac{1}{2} \frac{\partial}{\partial x} (\nabla^2 \omega) \right] + \frac{2}{3} Gh \left(\frac{\partial \omega}{\partial x} - \varphi_x \right) = 0$$

$$\frac{2D}{5} \left[(1-\mu) \nabla^2 \varphi_y + (1+\mu) \frac{\partial \phi}{\partial y} + \frac{1}{2} \frac{\partial}{\partial y} (\nabla^2 \omega) \right] + \frac{2}{3} Gh \left(\frac{\partial \omega}{\partial y} - \varphi_y \right) = 0 \quad \dots 9$$

Assuming the deflection and rotation displacement functions are given by:

$$\omega = \sum_{m=1}^{\infty} \sum_{n=1}^{\infty} A_{mn} \sin \frac{m\pi x}{a} \sin \frac{n\pi y}{b}$$

$$\varphi_x = \sum_{m=1}^{\infty} \sum_{n=1}^{\infty} B_{mn} \cos \frac{m\pi x}{a} \sin \frac{n\pi y}{b}$$

$$\varphi_y = \sum_{m=1}^{\infty} \sum_{n=1}^{\infty} C_{mn} \sin \frac{m\pi x}{a} \cos \frac{n\pi y}{b} \quad \dots 10$$

Plate boundary conditions have been fully met. Then, lateral load is continued to show double trigonometric series:

$$q(x, y) = \sum_{m=1}^{\infty} \sum_{n=1}^{\infty} q_{mn} \sin \frac{m\pi x}{a} \sin \frac{n\pi y}{b} \quad \dots 11$$

Considering formula (10) and formula (11), formula (8) can be written as:

$$B_{mn} = \left\{ 1 - \frac{3D\pi^2}{10Gh} \left[\left(\frac{m}{a} \right)^2 + \left(\frac{n}{b} \right)^2 \right] \right\} \times \frac{mq_{mn}}{aD\pi^3 \left[\left(\frac{m}{a} \right)^2 + \left(\frac{n}{b} \right)^2 \right]^2}$$

$$C_{mn} = \left\{ 1 - \frac{3D\pi^2}{10Gh} \left[\left(\frac{m}{a} \right)^2 + \left(\frac{n}{b} \right)^2 \right] \right\} \times \frac{nq_{mn}}{aD\pi^3 \left[\left(\frac{m}{a} \right)^2 + \left(\frac{n}{b} \right)^2 \right]^2} \quad \dots 12$$

As the roof is subjected to uniform load, with the increase of m, n , and the sharply decrease of q_{mn} , the effect on the deflection of roof is small, so when the $m=n=1$, it can ensure accuracy, Taking $m=n=1$ into formula (12), the value of A_{mn}, B_{mn}, C_{mn} can be obtained, then, take them into formula (10), the value of $\omega, \varphi_x, \varphi_y$ is got.

In the following, take the value of $\omega, \varphi_x, \varphi_y$ into formula (8), finally the value of M_x, M_y can be obtained, and the maximum value is got at $x = a/2, y = b/2$. According to the relationship between the maximum bending moment and stress, it can be written as:

$$M_{\max} = \frac{\sigma_s \times h^2}{6} \quad \dots 13$$

$$\sigma_s = \frac{6M_{\max}}{h^2} = \frac{6q_{11} \left(\frac{5}{a^2} + \frac{4\mu}{ab} + \frac{\mu}{b^2} \right)}{5\pi^2 \left(\frac{1}{a^2} + \frac{1}{b^2} \right)^2 h^2} + \frac{6q_{11}\mu \left(\frac{1}{b^2} - \frac{1}{ab} \right)}{25(1-\mu) \left(\frac{1}{a^2} + \frac{1}{b^2} \right)} \quad \dots 14$$

Where E is the modulus of elasticity, μ is the Poisson's ratio, v, u is the surface displacement, ω is the plate deflection, τ_{xz}^0, τ_{yz}^0 is shear stress in the plane transverse, D is the plate flexural rigidity ($D = \frac{Eh^3}{12(1-\mu^2)}$), G is the shear modulus ($G = \frac{E}{2(1+\mu)}$), is the thickness of the plate, ∇^2 is the Laplace operator.

According to the formula (14), the upper lamprophyres occur tensile bending damage and fracture when the parameters of the upper lamprophyre is $q_{11} = q_1 = 1.85\text{MPa}$, $\mu = 0.21$, $h = 20$ meters, $\sigma_s = 12\text{MPa}$, $b = 230$ meters. Input the formula (12) and the corresponding parameters into the MATLAB programming, the fracture length $a = 69.4$ meters is obtained.

3.2 THE LOWER LAMPROPHYRE CAVING STEP

The calculation of the lower lamprophyre fracture distance can use the thin plate theory[7]. Under uniformly distributed load, the boundary condition can be written as:

$$\begin{aligned} \omega|_{x=0} &= 0, \left(\frac{\partial^2 \omega}{\partial x^2} + \mu \frac{\partial^2 \omega}{\partial y^2} \right)_{x=0} = 0 \\ \omega|_{x=a} &= 0, \left(\frac{\partial^2 \omega}{\partial x^2} + \mu \frac{\partial^2 \omega}{\partial y^2} \right)_{x=a} = 0 \\ \omega|_{y=0} &= 0, \left(\frac{\partial^2 \omega}{\partial y^2} + \mu \frac{\partial^2 \omega}{\partial x^2} \right)_{y=0} = 0 \\ \omega|_{y=b} &= 0, \left(\frac{\partial^2 \omega}{\partial y^2} + \mu \frac{\partial^2 \omega}{\partial x^2} \right)_{y=b} = 0 \end{aligned} \quad \dots 15$$

The deflection surface equation can be written as:

$$\omega = A \sin \frac{\pi x}{a} \sin \frac{\pi y}{b} \quad \dots 16$$

The formula satisfies the above boundary conditions, and

$$\text{when, } \frac{\partial I}{\partial A} = 0$$

The A is govern by:

$$A = \frac{16q}{\pi^6 D \left(\frac{1}{a^2} + \frac{1}{b^2} \right)^2} \quad \dots 17$$

M_x can be written as:

$$M_x = -D \left(\frac{\partial^2 \omega}{\partial x^2} + \mu \frac{\partial^2 \omega}{\partial y^2} \right) \quad \dots 18$$

$$\text{so: } M_x = \frac{16q \sin \frac{\pi x}{a} \sin \frac{\pi y}{b} \left(\frac{1}{a^2} + \frac{\mu}{b^2} \right)}{\pi^4 \left(\frac{1}{a^2} + \frac{1}{b^2} \right)^2} \quad \dots 19$$

when $x = a/2, y = b/2$ the maximum can be written as:

$$M_{\max} = \frac{16q \left(\frac{1}{a^2} + \frac{\mu}{b^2} \right)}{\pi^4 \left(\frac{1}{a^2} + \frac{1}{b^2} \right)^2} \quad \dots 20$$

Combined with the (20) and (13):

$$\sigma_s = \frac{96q \left(\frac{1}{a^2} + \frac{\mu}{b^2} \right)}{\pi^4 \left(\frac{1}{a^2} + \frac{1}{b^2} \right)^2 h^2} \quad (21)$$

When meeting the formula (21), the lower lamprophyres occur tensile bending damage and fracture. The parameters of the lower lamprophyre is $q = q_2 = 0.158\text{MPa}$, $\mu = 0.21$, $h = 4$ meters, $\sigma_s = 12\text{MPa}$, $b = 230$ meters. To put the formula (21) and the corresponding parameters into the MATLAB programming, the fracture length $a = 35.8$ meters can be got.

According to the above analysis, the upper lamprophyre caving step distance is 69.4 meters, and the lower the lamprophyre caving step distance is 35.8 meters. Upper layer thickness lamprophyre fracture step distance of roughly is two times than the lower layer lamprophyre fracture step distance. Small roof weighting is formed when the lower lamprophyre primary fractured. Meanwhile, large roof weighting is formed when the upper lamprophyre fractured.

4. The roof caving of goaf gas transport model under impact

The gob is loose porous medium composed of coal and rock before roof caving, its permeability distribution and pore pressure are almost the same, the impact force of roof caving will affect the permeability distribution and flow field in gob [14]. The vertical force component of impact force can instantly effect on point of goaf coal and gangue compaction when the roof caving, the horizontal force component of the impact force can not only compress the left coal and gangue in the horizontal direction of the goaf and increase the goaf gas pressure in porous media, but also format "blowing" effect on gas in goaf to provide the power source for gas emission in goaf. The impact of roof caving on the porous medium is an important factor of the gas emission in the working face, and the different roof caving will cause different effects on the gas emission in goaf.

The main emission way of gob gas is the high extracted

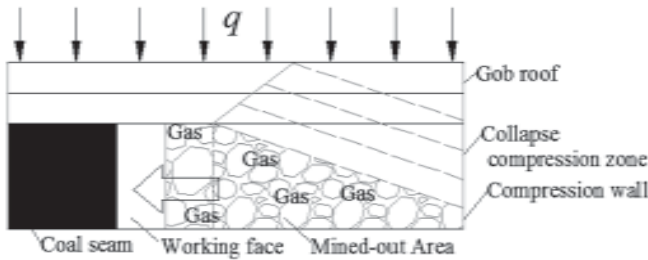


Fig.4 Influence of roof falling to gob

way. By measuring the resistance of the bracket and the change of gas concentration, it can be very good to reflect the roof caving rule and the influence of the gas emission in the goaf. In the normal production process, high extracted way is less affected by human factors because of its location, so it can be a very good reaction of gob gas emission changes. The corresponding relationship between the gas concentration of the high extracted way and the weighted average resistance of the support is shown in Fig.5

Fig.5 shows that the working face support resistance has large and small periodic variation, and the gas concentration and support resistance showed good correspondence, large pressure cycle for 11~13 days, small pressure cycle 6~7 days, the working surface on advance of 5.6m/d, so the mining step are 61.6 ~ 72.8 meters and 33.6 ~ 39.2 meters. According to the third chapter of theoretical analysis and calculation of roof caving step, the support resistance and gas concentration change are consistency. The relationship between the pressure and fracture length and the corresponding gas emission can be verified.

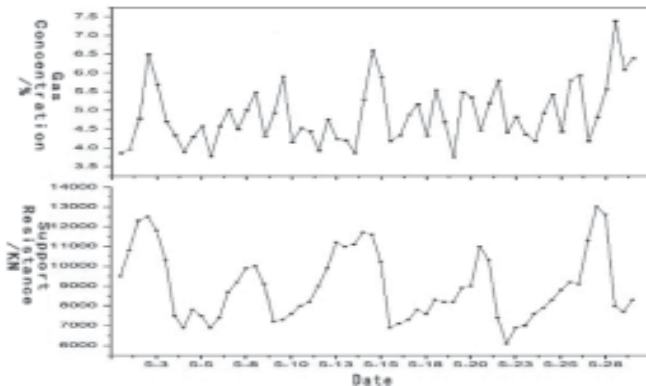


Fig.5 High alley pumping the gas concentration and stent weighted average resistance corresponding diagram

5. Layered hard roof breaking mining goaf gas migration numerical solution and analysis of the fault

5.1 THE GAS FLOW MODEL OF WORKING FACE

The impact force of roof falling across the goaf is the main cause of the deformation of the frame and the void of the porous medium. In the compression process, the goaf gas pore pressure gradually increased, resulting in goaf gas flocking into the working face instantly [15]. In order to study

the shape of gas flow field in the gob roof caving, the following assumptions are made: roadway and working face in coal mine is a pipeline flow, the gob is the porous medium of coal and waste rock, coal rock solid skeleton is compressible, and the compression of free gas in the void during the deformation process is isothermal compression, it meets the ideal gas equation, gas saturation of coal and rock mass, and the moment of gas desorption is completed.

5.1.1 Working surface flow equation

The Navier-Stoke equation can describe the flow pattern of the fluid in the pipeline well, both the breeze and the turbulence can be solved by the Navier-Stoke equation, in this paper the Navier-Stoke equation is used as the working surface air flow control equation:

$$-\nabla \cdot \eta \left(\nabla u_{ns} + (\nabla u_{ns})^T \right) + \rho u_{ns} \cdot \nabla u_{ns} + \nabla p_{ns} = 0 \quad \dots 22$$

$$\nabla \cdot u_{ns} = 0 \quad \dots 23$$

In this formula, η is defined as the viscosity coefficient, $\text{kg}/(\text{m} \cdot \text{s})$; μ is the velocity vector, ρ is the liquid density, kg/m^3 ; p is the pressure. The dependent variables of the Navier-Stokes equation are velocity (μ) and pressure (p), subscript "ns".

5.1.2 Ideal gas and porosity equation

$$\phi_2 = \frac{V_1' - V_0}{V_1' P_1} = \frac{\phi_1 V_1' - V_0}{V_1' P_1} = \frac{\phi_2 V_2' - V_0}{V_2' P_2} \quad \dots 24$$

$$\phi_2 = \frac{V_1' - V_0}{V_1' P_1} = \frac{\phi_1 V_1' - V_0}{V_1' P_1} = \frac{\phi_2 V_2' - V_0}{V_2' P_2} \quad \dots 25$$

$$pV = nRT \quad \dots 26$$

$$\dots 27$$

Where ϕ_1 , η_2 are the porosity of the porous medium before and after compression, respectively. V_0 is the volume of coal solid skeleton, m^3 . V_1' , V_2' are the void volume before and after the deformation of coal rock, respectively, m^3 . P is the methane gas pressure, MPa . V is the volume of methane gas, m^3 . n is the amount of substance of idea gas, mol. R is the universal gas constant, $8.31 \text{ J}/(\text{mol} \cdot \text{K})$. T is the gas temperature, K . p_1 and p_2 are the gob roof collapse pore pressure before and after the fall, respectively, MPa .

5.1.3 Seepage equation

The porosity and permeability of the porous media are related to the stress state in the porous medium, as:

$$\phi = (\phi_\sigma - \phi_0) e^{(\alpha\sigma)} + \phi_0 \quad \dots 28$$

$$\sigma = (\sigma_x + \sigma_y) / 2 \quad \dots 29$$

$$k = \frac{d^2}{150} \frac{\phi^3}{(1-\phi)^2} \quad \dots 30$$

Where ϕ , ϕ_{σ} , ϕ_0 are the Porosity of porous medium, porosity under load σ , porosity under high compression ratio, respectively. α is the permeability stress sensitivity coefficient, $5.0 \times 10^{-8} Pa^{-1}$. k is permeability in porous media, m^2 . d is the particle size of porous media, mm.

5.2 THE CALCULATION MODEL AND PARAMETERS

Computing gas pressure and concentrating changes of Tashan 8214 caving mining face under the 3D state of roof caving according to coal seam roof lithology and cross breaking step. Liang Yuntao [16] built the model of medium porosity and permeability of caving non uniformly continuous distribution. According to the conclusion, we set the gob area initial porosity was 0.4. The lower lamprophyre cross fault step distance is 40m, the upper lamprophyre cross fault step distance is 70m. So we building model according to the actual, the model only considers the gas emission in the gob, and ignores the gas emission in the coal wall of the working face. When the lower lamprophyre broken (Fig.6), the roof load q_1 is 0.158MPa, gob height 12 meters, working face air inlet 3600m³/min. When the upper lamprophyre broken (Fig.7), the roof load q_2 is 1.85MPa, gob height 20 meters, working face air inlet 3600m³/min.

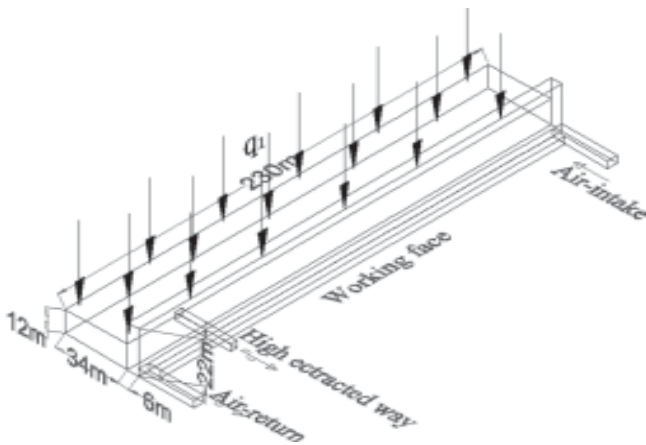


Fig.6 Lamprophyre lower goaf collapse under the effect of the calculation model

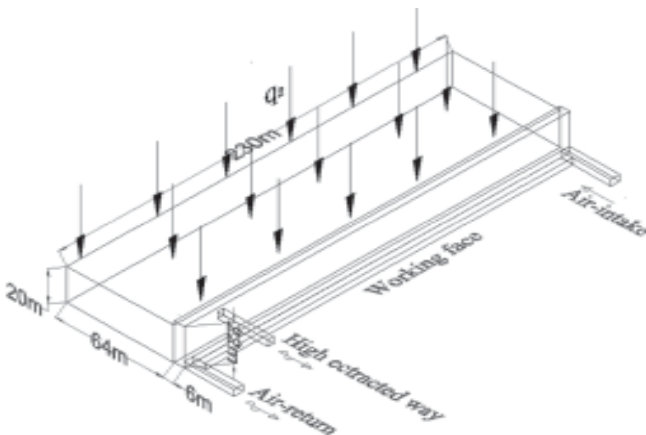


Fig.7 Lamprophyre upper goaf collapse under the effect of the calculation model



Fig.8 The gas concentration profile of computing model at different times

5.3 CALCULATION RESULTS AND ANALYSIS

Through the analysis, the impact force of roof caving mainly changes the state of goaf gas flow field within a certain time, goaf gas flow state determines the methane concentration of the return airway and the upper corner. So it is important to study the gas flow field under the action of the roof falling impact force. According to the above assumptions and control equations, the gas concentration distribution map of different time under the influence of roof falling can be obtained by numerical calculation. The results are shown in the figures below.

1. The calculation results of the goaf gas emission by the effect of lower lamprophyre broken.
2. The calculation results of the goaf gas emission by the effect of upper lamprophyre broken.

Figs. 8 and 10 shows that the moment of the roof falling squeeze the goaf makes the gob methane flooding into the working face in a short period of time, which causes the upper corner, return airway and high extracted way gas concentration increasing rapidly. To monitor the methane concentration on the corner, return airway and high drainage roadway, the gas concentration change curve as Figs. 9 and 11 can be got. It indicates that the maximum concentration of the upper corner, return airway and high extracted way are 4.8%, 3.4% and 5.6%, respectively when the lower lamprophyre fracture. Figure 10 shows that the maximum concentration of the upper corner, return airway and high extracted way are 9.3%, 6.1% and 8.3%, respectively, when the upper lamprophyre fracture.

The goaf is composed of porous media by coal gangue. In the upper strata caving process of goaf compaction, the goaf tends to gradually achieve a balanced state, and the gas emission tends to be stable, the upper corner, return airway and high drainage roadway gas concentration reach the peak values, then gradually decrease to normal state. Analyzing the strata location and caving step distance, it can be found that

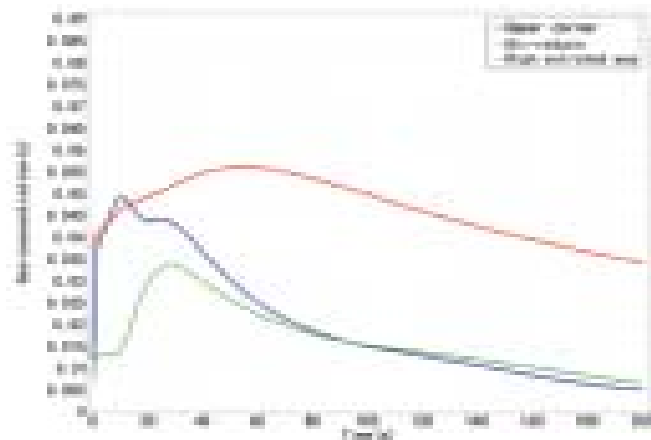


Fig.9 Gas concentration curve of high extracted way, upper corner and return airway after shock effect roof collapse



Fig.10 The gas concentration profile of computing model at different times

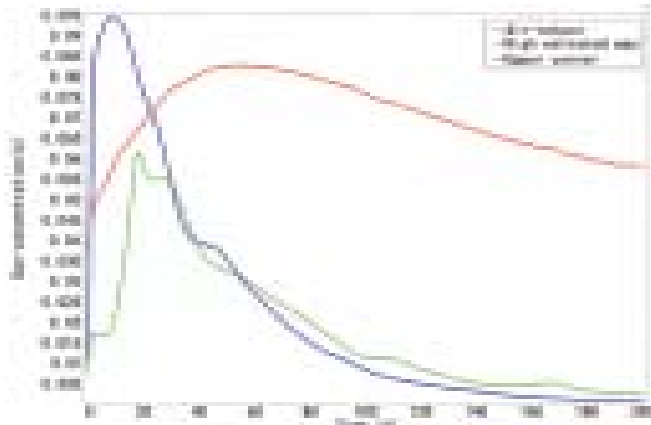


Fig.11 Gas concentration curve of high extracted way, upper corner and return airway after shock effect roof collapse

the upper lamprophyre bearing the goaf's volume is three times than lower lamprophyre, and the roof load is much larger than the lower lamprophyre, the process of caving goaf causes a greater degree of disturbance, which leads to more gas emission.

6. Conclusions

Based on the Vlasov thick and thin plate theory, this paper gets the breaking span of hard rock strata which are quite different in thickness in a near distance in Datong mining area. The results show that the upper roof breaking span is 69.4 meters, the lower roof breaking span is 35.8 meters, and the breaking span of the upper roof is twice longer than the lower one.

As we can see from the face support resistance curve, the value of support resistance shows-periodic variation. To the advancing speed, the corresponding step is 61.6 ~ 72.8 meters and 33.6 ~ 39.2 meters. And the calculation results are consistent with the field observation.

The calculation model of dynamic gas migration in goaf under the influence of different hard roof caving based on the thick seam hard roof breaking rules is established. By using multiphysics coupling calculation, the gas migration law in goaf under the effect of different roof pressure is revealed. The results show that the goaf methane rapidly move to the working surface and the return air side with the impact of the roof caving, which leads to the upper corner and return airway methane gas overrunning. Comparing the concentration variation of different stratum roof breaking off monitoring points, we can draw a conclusion that the upper thicker hard roof fracture causes more amounts of gas emission than the lower roof. When the upper roof caving, the gas concentration in the upper corner jump range is especially striking, which is more likely to cause the gas disaster, so that we should focus on the goaf and the gas in upper corner, and stress on prevention and control the large area whole caving goaf roof.

Reference

- [1] Wang H. Y., Cheng Y. F., Yu B. (2015): Adsorption Effect of Overlaying Strata on Carbon Dioxide in Coalfield Fire Area. *International Journal of Heat and Technology*, 33(3): 11-18.
- [2] Yu B. (2014): Study on Strong Pressure Behavior Mechanism and Roof Control of Fully Mechanized Top Coal Caving in Extra Thickness Seam in Datong Coal Mine. Ph.D. dissertation, China University of Mining and Technology, Xuzhou.
- [3] Li B. Y., Zhang N. (2014): Stability Analysis and Controlling Scheme Optimization On Roadway Driven Along Goaf of Fully Mechanized Top Coal Caving. *Env and Earth Sci Res J*, 1(1):17-22.
- [4] Meng X. R., Zhang W. C., He Y. Q. (2006): Study of gas emission characteristic in long-wall top coal caving face with a high gas content. *Journal of Mining & Safety Engineering*, 23(4): 419-422.
- [5] Wang J. C., Wang Z. H. (2015): Stability of main roof structure during the first weighting in shallow high-intensity mining face with thin bedrock. *Journal of Mining & Safety Engineering*, 32(2): 175-181.
- [6] Li S.G., Lin H.F., Cheng L.H. (2004): Relation between abutment pressure and relieved gas delivery for fully-mechanized top coal caving. *Chinese Journal of Rock Mechanics & Engineering*, 23(19): 3288-3291.
- [7] Jia X. R. (2010): Rock mechanics and rock strata control. Beijing, China: China University of Mining and Technology Press, 258-269.
- [8] Tang X. L., Ye M. L. (2003): The Thin Plate Theory Analysis of Hard Roof and Pressure Forecast. *West-china Exploration Engineering*, (8):67-69.
- [9] Tu H. S., Tu S. H., Chen F. Study on the deformation and fracture feature of steep inclined coal seam roof based on the theory of thin plates. *Journal of Mining & Safety Engineering*, 31(01): 49-55.
- [10] Weng M. Y., Xu J. H., Li C. (2011): Relationship of coal and rock damage underground behavior and methane gushing in fully-mechanized caving mining face. *Meitan Xuebao/journal of the China Coal Society*, 36(10): 1709-1714.
- [11] Li H.M., Wang W., Xiong Z. Q. (2008): Relationship between mining induced surrounding rock movement and gas emission in working face. *Journal of Mining & Safety Engineering*, 25(1): 11-16.
- [12] Qian M.G., Liao X.X., Xu J.L. (2003): Key strata theory of strata control. Beijing, China: China University of Mining and Technology Press.
- [13] He F.B., Shen Y.P. (1993): Theory of plates and shells. Xi'an, China: Xi'an Jiao Tong University Press, 182-187.

- [14] Hao T.X., Jin Z.C., Li F. Optimization of Goaf Gas Drainage Parameters Based on Numerical Simulation Studying Fracture in Overlying Strata. *Procedia Engineering*, 43(9): 269-275.
- [15] Al-khliefat V.M., Duwairi H.M. (2015): Darcian velocity and temperature jump effects on convection from vertical surface embedded in porous media. *International Journal of Heat and Technology*, 33(2): 97-102.
- [16] Liang Y.T., Zhang T.F., Wang S.G., Sun J.P. (2009): Heterogeneous model of porosity in gobs and its airflow field distribution. *Journal of the China Coal Society*, 34(9): 1203-1207.